3.12

VISUALIZATION TECHNIQUES FOR APPLICATIONS OF HIGH-RESOLUTION NUMERICAL WEATHER MODELS

Lloyd A. Treinish* and Zaphiris D. Christidis
IBM Thomas J. Watson Research Center, Yorktown Heights, NY

1. INTRODUCTION

Visualization is a method of computing by which the enormous bandwidth and processing power of the human visual (eye-brain) system becomes an integral part of extracting knowledge from complex data. In that regard, our previous work has discussed methods of appropriate mapping of user goals to the design of pictorial content by considering both the underlying data characteristics and the (human) perception of the visualization (Treinish, 1999). However, the scaling of traditional data sources and introduction of new applications challenges the effectiveness of conventional visualization methods. Consider, for example, rapid execution (e.g., 10 to 30 times faster than real-time) of mesoscale weather models operating at cloud-scale resolution. Earlier we illustrated that there is a mismatch between this rate of data generation and the ability to utilize the model results with traditional two-dimensional techniques (Treinish and Rothfusz, 1997). Introduction of three-dimensional visualization is only a partial solution because typical methods can easily fail to capture the salient characteristics of such simulations.

2. APPROACH

The resolution of the visualization must match that of the scale of the model to build usable products that are perceptually coherent. We have determined that realization needs to be based upon the integration of all computational nests with high-resolution topography in a three-dimensional cartographic coordinate system and sequencing consistent with the internal time step of the computation. The choice of realization geometry is also affected by the resolution of the data so that perceptual artifacts do not dominate the presentation, especially in animation (Treinish, 1999). We have looked at problems with visualization of these model results for typical meteorological operations as well as applications in other domains.

3. VECTOR FIELD REALIZATION

The choice of realization methods is particularly important for vector fields (e.g., predicted winds). We have used several techniques for wind velocity, which are pseudo-colored by speed. For ground level data, we typically drape the results over a topographic surface. A continuous colormap is used ranging from a deep violet or green, for example, for very calm winds to white for the maximum speed. Such a luminance-based colormap is perceptually isomorphic for data with relatively high spatial frequency (Rogowitz and Treinish, 1998). Vector arrows are a common technique, but we create them with fixed size to eliminate misleading motion cues during animation. Similar problems would also occur in animation if wind barbs are employed, which are best suited for static displays. Fixed size arrow glyphs are illustrated in Figure 1. It shows the result of a mesoscale forecast generated by the Regional Atmospheric Modeling System (RAMS). The domain is at 6.5 km resolution in a region roughly 650 x 650 km in extent to include Hawaii (cf., Snook et al, 1998). Output from RAMS every 10 minutes of forecast time are generated for a browsing visualization (Treinish, 1999).

*Corresponding author address: Lloyd A. Treinish, IBM T. J. Watson Research Center, P. O. Box 704, Yorktown Heights, NY 10598, lloydt@us.ibm.com, http://www.research.ibm.com/people/l/lloydt

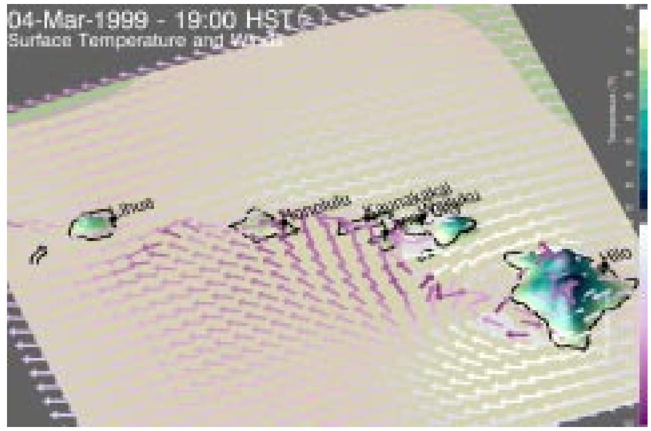

Figure 1. Predicted Winds Visualized as Arrow Glyphs with Temperature Contours and a Terrain Surface.

The image shows a terrain map as a deformed surface, pseudo-colored by color-filled contour bands of predicted temperature overlaid with coastline maps for 7 PM local time on March 4, 1999. This approach generates a textured field, which is effective at showing gross predicted atmospheric movement. The visualization is consistent with prevailing wind patterns in Hawaii. However, this structure is disturbed on the lee side of the big island of Hawaii and to a lesser extent, Maui.

Unfortunately, this realization technique does not capture sufficient details to interpret these apparent features. Instead, we introduce streamlines with directional arrows. Although visually more complex they are superior at capturing fronts, convergence zones, vortices, etc. An example result for the same forecast period is shown in Figure 2. The temperature data are now shown as a continuous field as better contrast with the wind visualization. A perceptually isomorphic colormap is used between opposing saturation pairs for such low-spatial frequency data.

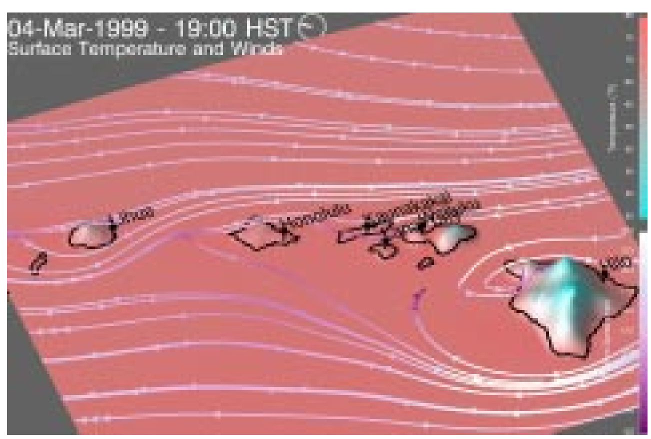

Figure 2. Predicted Winds Visualized as Streamlines with a Terrain Surface Colored by Temperature.

The results show more fine structure, but there are gaps, especially in regions that potentially are interesting as implied in Figure 1. The problem is that a conventional approach toward steady-state streamline generation was used. In particular, the domain was uniformly sampled to define seed points for integration. While generic, it fails to capture salient high-resolution features. This is a well-known issue in flow visualization utilized in aerospace computational fluid dynamics (e.g., Helman and Hesselink, 1990). A key problem in these applications is the understanding of the topology of the underlying vector field. Among the more important characteristics of the topology are the location of critical points (i.e., where the velocity field vanishes) and tangent curves, which connect these points. To first order, we can identify the location of the critical points by the eigenvectors and eigenvalues of the divergence of the velocity. In particular, we use a sampling of the locations where the divergence is zero as seed points for integration. The resultant streamlines are thus, an approximation of tangent curves. To ensure consistency in this steady-state calculation for animation, this determination is done for each time step. An application of this approach for the previously used forecast period is shown in Figure 3.

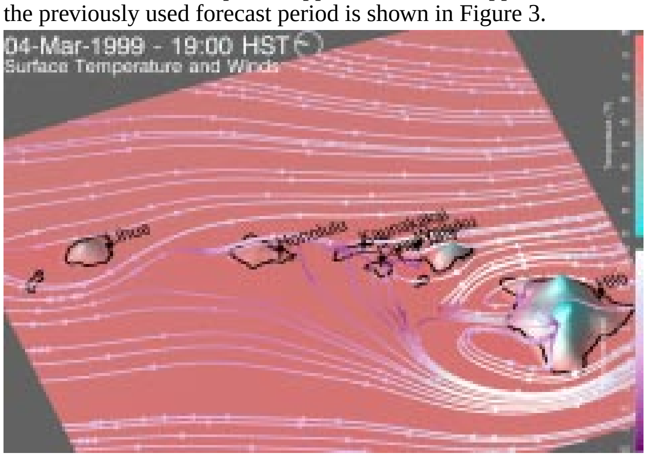

Figure 3. Wind Streamlines as Tangent Curves Using Critical Point Determination.

The technique is clearly superior at capturing detailed features from the high-resolution forecast. In this case, the structure of the wind field on the lee side of the islands is now clear. This morphology is due to vortex shedding of the fluid flow past mountains not unlike what can happen behind a wing or an engine nacelle for a jet aircraft in flight. The results are particularly compelling when animated by time. This technique looks promising for the visualization of other high-resolution orographic effects on predicted winds.

An improved initial representation of predicted winds enables one to identify features of potential interest for further analysis. We have introduced several additional approaches to study the data in greater detail. The first is to incorporate both spatial and temporal integration as streaklines. Another is to examine other predicted fields generated by the model in conjunction with wind data. Figures 4 and 5 show examples of this idea, fusing multiple variables into a consistent representation (Treinish, 1999). They are for the same forecast period depicted in Figures 1, 2 and 3. Figure 4 illustrates a surface variable (precipitable water) for display as pseudo-colored filled contour bands, which are overlaid on a topographic map. Coastlines (black) are draped on the surface. An upper air variable (relative humidity) is displayed via surface extraction.

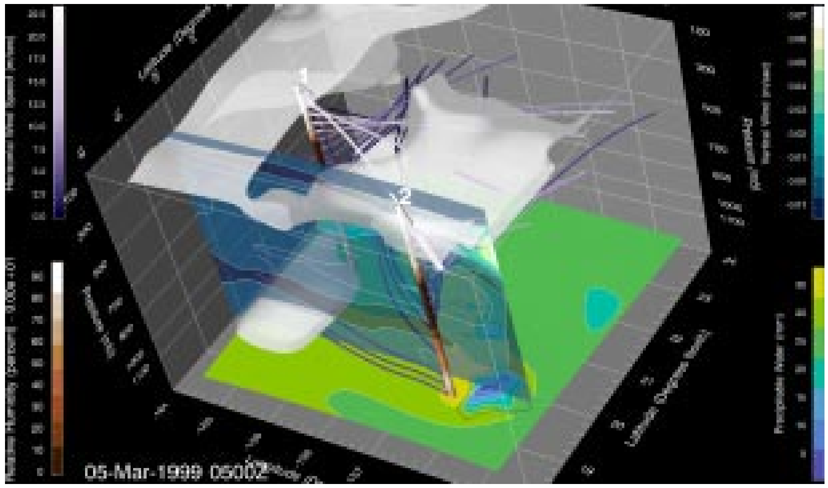

Figure 4. Three-Dimensional Wind Streamlines with Surface and Upper Air Data.

The surface at 90% is requested in translucent white, which corresponds roughly to a cloud boundary. Another field (vertical wind speed) has been selected to show as a vertical slice, which is pseudo-color contoured. The location of the slice was chosen to include the area at the lee of Hawaii as identified in Figure 3. The upper air wind data can be seen along two vertical profiles, which are specified interactively to study this same area. The direction of the model wind field along these "virtual soundings" is shown via vector arrows and streamribbons. Both the arrows and ribbons are pseudo-colored by horizontal wind speed. The length of the arrows also corresponds to the horizontal speed. Points along the profile are used as seeds for the streamribbon integration. Each profile is realized as a pseudo-colored tube, which is contoured by the variable selected for isosurface realization (i.e., relative humidity). The visualization for the profile marked 2 can help illustrate the upper air characteristics of the predicted vortex shedding described earlier.

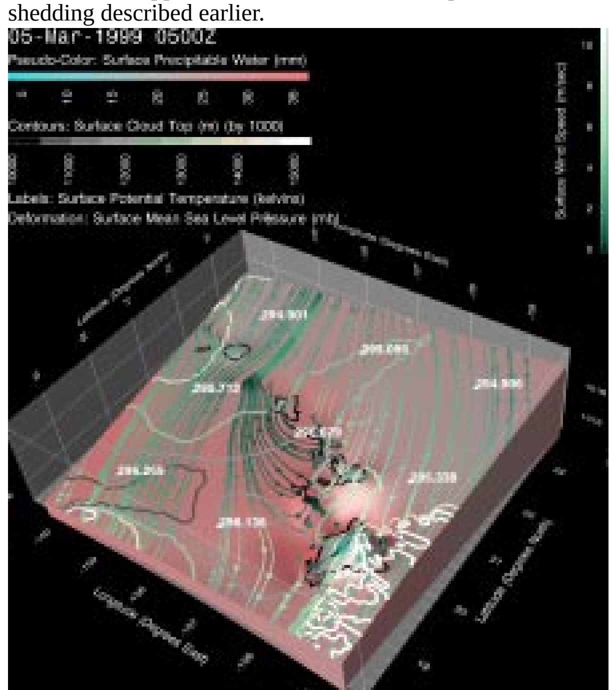

Figure 5. Integration of Wind Streamlines with Other Surface Variables.

Figure 5 shows another approach in which five different surface variables have been selected in a combined visualization. Precipitable water is shown as pseudo-color. Wind velocity is illustrated as streamlines, colored by speed, using the same technique as in Figure 3. Colored line contours of cloud top heights in increments of 1000 m are shown. Each of these planar representations are deformed vertically by mean sea level pressure to create a shaded surface. A coastline map (black) is draped on the surface. Finally, temperature values at discrete locations are also shown by value on the surface. One can see the distinctions between the leeward and windward sides of the islands in this representation, particularly for the large island of Hawaii. The effect of the vortex shedding on cloud heights is also apparent.

4. APPLICATIONS

We have extended our earlier work for situations where high-resolution models can be utilized in variety of decision-making efforts such as emergency planning, energy production, airline operations, risk assessment, etc. These applications imply the coupling of weather simulations with other models, analyses and data. To enable effective assessment and appropriate decisions, focused visualizations must be designed to integrate these distinct data sources, yet still be driven by user goals. This leverages our past efforts in providing uniform access to a diversity of data by preserving their underlying fidelity despite variations in sampling and coordinate systems (Treinish, 1994). In many cases, the resultant visualizations do not show forecasts of weather phenomena directly but the derived properties, which are influenced by weather. These ideas are illustrated by two examples.

4.1 Demographics

In many applications, the design of a visualization should be based upon the correlation of weather prediction with other sources of data relevant to decision making. This is illustrated in Figure 6, which shows the relationship between demographic data and a forecast generated by RAMS. The domain in this example is 800 x 800 km at 8 km resolution centered over Dallas.

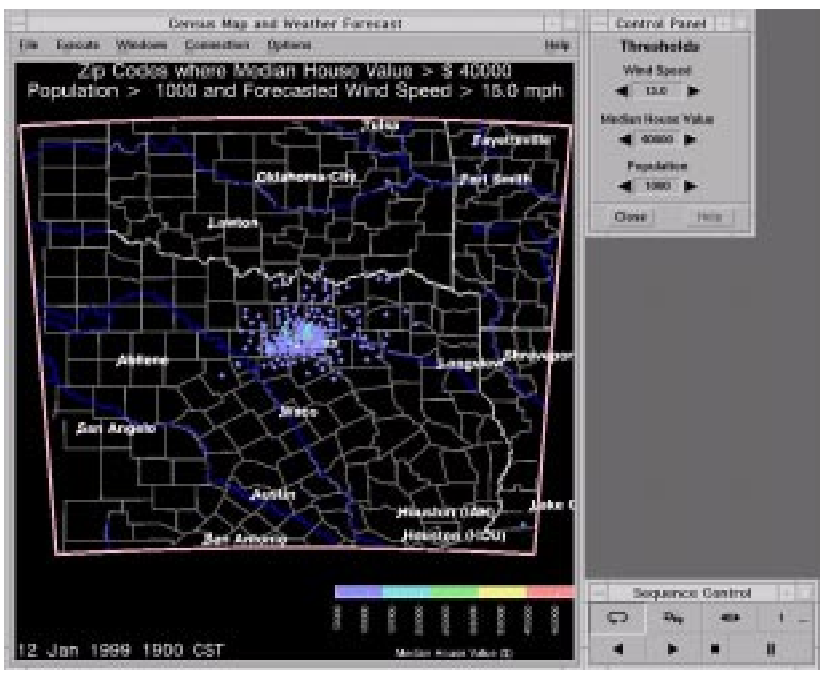

Figure 6. Correlation of a weather forecast with demographic data.

The forecast was generated in real-time during the 1999 AMS conference in the exhibition area. In this case, the visualization is a simple two-dimensional map, which shows a set of glyphs, colored by median house value. The glyphs are located at the centroid of the area associated with zip codes in the forecast domain. These locations are only marked on the map when a set of conditions on house value, population and predicted wind speed are met, as indicated in the control panel widget. The demographic data are derived from available census information (`http://tiger.census.gov`). The user is free to interactively set these thresholds and animate the results in time corresponding to the weather simulation in hourly steps. These thresholds can be augmented to include other relevant demographic, customer or property data. Essentially, they represent a simple method to specify a query into various static and dynamic data sets, which are then used to constrain a visual integration for display and interaction. Such an application may be useful for planning purposes by an insurance company or deployment of repair crews by a utility.

4.2 Energy Load Forecasting

In other cases, the results from the simulation need to be coupled to other models. In agriculture, that could include an hydrological model to evaluate the effect of runoff from predicted rainfall to help understand the impact on the application of pesticides and fertilizer or planting of new seed. In the energy industry, it would typically be input to a model used to predict load on a power-generation facility or transmission lines for efficient running of the facility or for trading. This idea is illustrated in Figure 7. It shows a map of Georgia with forecasted heat indices at 8 km resolution generated by RAMS. Major cities and locations of the generators owned and operated by Georgia Power, the local electricity utility, are shown by name. Each power plant location is also marked with a pin. The height and color of the pin indicate an estimated load.

The load is computed interactively as a function of temperature and time of day from a simple model. The temperature dependence is based upon a polynomial approximation of the relationship between historical data of power demand and weather observations (Robinson, 1996). The temporal variation is based upon a spline fit of hourly electricity requirements for mid-week days in an urban tropical environment, which is consistent with other results in the literature (Chang and Yi, 1998). The function is scaled by the rated power plant capacity using published data (`http://www.georgiapower.com/newsroom/plants.asp`). Heat index is used as a more accurate measure of demand than simply temperature. The weather model results are interpolated at each time step to the location of each of the power plants. In the interactive application, the user has the ability to select the type of power plant (fossil, hydroelectric and/or nuclear), what data to show on the map (e.g., weather, geographic or other customer/demographic) and to query individual power plants. The results of the query include the predicted load at each time step (as fine as every 10 minutes) as well as a plot of predicted load over 24 hours with weather data at that location.

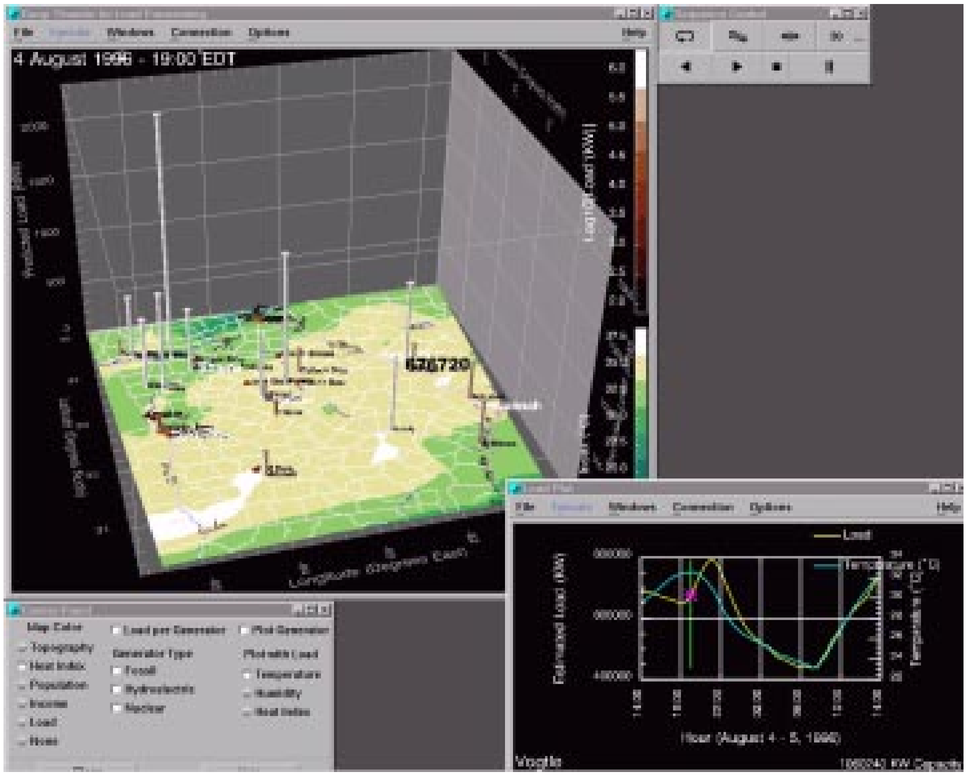

Figure 7. Correlation of a weather forecast with load prediction.

The latter may indicate more precisely regions of separation or attachment of predicted wind fields.

The visualization of applications of mesoscale modeling have benefited from a focus on specialized interfaces and tools matched to user goals and underlying visualization tasks. We believe that this idea can be extended to other application areas such as agriculture, aviation, emergency planning, etc. Within any given application, incorporation of additional and more complex data sets will also be addressed. Our goal is to develop simple interfaces and useful visual fusion.

5. IMPLEMENTATION

Figures 1 through 5 were generated by the visualization component of an integrated operational mesoscale numerical weather prediction system. Additional information about the system as well as numerous visualization examples are available at **`http://www.research.ibm.com/weather`**. They present a user interface based upon XWindow/Motif for indirect interaction and OpenGL for direct three-dimensional interaction in cartographic coordinates. They have been implemented with Visualization Data Explorer (DX) (Abram and Treinish, 1995).

DX is a portable, general-purpose software package for visualization and analysis. A generic toolkit was used to avoid having to implement a graphics and computational infrastructure. Unlike traditional meteorological graphics, DX is parallelized for multiprocessor workstations and can utilize three-dimensional graphics accelerators. DX is built upon an unified data model that enables these applications to operate directly on the native grids without transformation or compression, which preserves the fidelity during visualization (Treinish, 1994). Further, such a toolkit is extensible to allow development to be focused on meteorological data, applications and tasks, and reuse of tools between applications with similar user interface components. Hence, new applications as illustrated in Figures 6 and 7 required no additional infrastructure development.

6. CONCLUSIONS AND FUTURE WORK

Adaptation of on-going work in computational flow visualization looks promising in applications to high-resolution numerical weather models. As the complexity of the underlying meshes increases to accommodate orographic and other effects in detail, we will utilize additional methods for improved global representation such as line integral convolution and critical point analysis for tangent curve classification.

7. REFERENCES

Abram, G. and L. Treinish. *An Extended Data-Flow Architecture for Data Analysis and Visualization*. **Proceedings of the IEEE Visualization 1995 Conference**, October 1995, Atlanta, pp. 263-270. (DX is now available as open source software via `http://www.research.ibm.com/dx` and `http://www.opendx.org`**)**

Chang, C. S. and M. Yi. *Real-Time Pricing Related Short-Term Load Forecasting*. **Proceedings of the Energy Management and Power Delivery 1998 Conference**, March 1998, Singapore, pp. 411-416.

Helman, J. L. and L. Hesselink. *Surface Representations of Two- and Three-Dimensional Fluid Flow Topology.* **Proceedings of the IEEE Visualization 1990 Conference**, October 1990, San Francisco, pp. 6-13.

Robinson, P. J. *Modeling Utility Load and Temperature Relationships for Use with Long-Lead Forecasts*. **Journal of Applied Meteorology**, **36**, no. 5, May 1997, pp. 591-598.

Rogowitz, B. and L. Treinish. *Data Visualization: The End of the Rainbow.* **IEEE Spectrum**, **35**, no.12, December 1998, pp. 52-59.

Snook, J. S., P. A. Stamus, J. Edwards, Z. Christidis, J. A. McGinley. *Local-Domain Mesoscale Analysis and Forecast Model Support for the 1996 Centennial Olympic Games*. **Weather and Forecasting**, **13**, no. 1, 1998, pp. 138-150.

Treinish, L. *Visualization of Disparate Data in the Earth Sciences*. **Computers in Physics**, **8**, n.6, November/December 1994, pp. 664-671.

Treinish, L. *Creating Effective Visualizations for Operational Weather Forecasting*. **Proceedings of the 15th IIPS Conference**, January 10-15, 1999, Dallas, pp. 517-520.

Treinish, L. and L. Rothfusz. *Three-Dimensional Visualization for Support of Operational Forecasting at the 1996 Centennial Olympic Games*. **Proceedings of the 13th IIPS Conference**, February 2-8, 1997, Long Beach, pp. 31-34.